Nuclear Operating Company
South Texas Project Electric Generating Station P.O. Box 289 Wadsworth, Texas 77483

December 4, 2008
U7-C-STP-NRC-080067

U. S. Nuclear Regulatory Commission
Attention: Document Control Desk
One White Flint North
11555 Rockville Pike
Rockville, MD 20852-2738

South Texas Project
Units 3 and 4
Docket Nos. 52-012 and 52-013
Commitment Related to Tsunami Effects and Response to Request for Additional Information

Reference: Letter, M. A. McBurnett to Document Control Desk, "Submittal of Combined License Application Revision 2," dated September 24, 2008 (ABR-AE-08000073)

Attached are responses to NRC staff questions included in Request for Additional Information (RAI) letter number 35, related to Combined License Application (COLA) Part 2, Tier 2, Section 2.4S.6. This submittal includes responses to RAI question numbers 02.04.06-1, 02.04.06-2, and 02.04.06-3, and comprises a complete response to RAI letter number 35. In conjunction with preparing the response to RAI question 02.04.06-1, STPNOC satisfied Commitment # 5 related to resolution of docketing issues (see referenced letter).

Commitment #5 required a review of "The Current State of Knowledge Regarding Potential Tsunami Sources Affecting U.S. Atlantic and Gulf Coasts," and an update of FSAR Subsection 2.4S.6. This review has been completed, and included the most recent information in "Tsunami Hazard Assessment at Nuclear Power Plant Sites in the United States of America," Prasad, R. and Pacific Northwest National Laboratory (PNNL), NUREG CR-6966, PNNL-17397, NRC, Draft Report for Comment, Revision: August 2008 (ML082810348). Changes to FSAR Subsection 2.4S.6 resulting from this review, consistent with the response to RAI question 02.04.06-1, will be incorporated into the next routine revision of the COLA. This satisfies the requirements of Commitment #5.

When a change to the COLA is indicated in the response to an RAI, the change will be incorporated into the next routine revision of the COLA following NRC acceptance of the RAI response.

There are no commitments in this letter.

If you have any questions regarding these responses, please contact me at (361) 972-7136, or Bill Mookhoek at (361) 972-7274.

D091
NRO

STI 32404915

I declare under penalty of perjury that the foregoing is true and correct.

Executed on 12/4/08

Scott Head
Manager, Regulatory Affairs
South Texas Project Units 3 & 4

rhb

Attachments:

1. Response to Question 02.04.06-1
2. Response to Question 02.04.06-2
2. Response to Question 02.04.06-3

cc: w/o attachment except*
(paper copy)

Director, Office of New Reactors
U. S. Nuclear Regulatory Commission
One White Flint North
11555 Rockville Pike
Rockville, MD 20852-2738

Regional Administrator, Region IV
U. S. Nuclear Regulatory Commission
611 Ryan Plaza Drive, Suite 400
Arlington, Texas 76011-8064

Richard A. Ratliff
Bureau of Radiation Control
Texas Department of State Health Services
1100 West 49th Street
Austin, TX 78756-3189

C. M. Canady
City of Austin
Electric Utility Department
721 Barton Springs Road
Austin, TX 78704

*Steven P. Frantz, Esquire
A. H. Gutterman, Esquire
Morgan, Lewis & Bockius LLP
1111 Pennsylvania Ave. NW
Washington D.C. 20004

*George F. Wunder
*Tekia Govan
Two White Flint North
11545 Rockville Pike
Rockville, MD 20852

(electronic copy)

*George Wunder
*Tekia Govan
Loren R. Plisco
U. S. Nuclear Regulatory Commission

Steve Winn
Eddy Daniels
Joseph Kiwak
STP 3&4 Investments LLC

Jon C. Wood, Esquire
Cox Smith Matthews

J. J. Nesrsta
R. K. Temple
Kevin Pollo
L. D. Blaylock
CPS Energy

RAI 02.04.06-1:

QUESTION:

Section C.I.2.4.6.1 of Regulatory Guide 1.206 (RG) provides specific guidance with respect to the establishment of the probable maximum tsunami (PMT). This includes how the orientation of the site relative to the generating mechanism, shape of the coastline, offshore land areas, hydrography, and stability of the coastal area (proneness of sliding) were considered in the analysis. [Item 1] Provide an assessment (e.g., tsunami modeling analysis) of the East Breaks landslide to clarify whether the 7.6 m offshore wave height indicated by Trabant et. al. (2001) can be discounted. [Item 2] In addition, provide an assessment of other regions in the Gulf of Mexico prone to landslides. [Item 3] To independently validate whether no tsunami hazard exists for the proposed site, provide geologic methods and tsunami identification criteria used to justify the determination that no tsunami deposit was found at the site. [Item 4] Provide excavation photos from Units 1 and 2. [Item 5] Indicate if there are geologically conducive locations for the deposition and preservation of tsunami deposits at the STP site or nearby regions.

RESPONSE:

RAI Question 02.04.06-1 has been separated into five items. Item numbers are notated in the question above with brackets (e.g., "[Item 1]"). A response to each item is provided below.

[Item 1] *Provide an assessment (e.g., tsunami modeling analysis) of the East Breaks landslide to clarify whether the 7.6 m offshore wave height indicated by Trabant et. al. (2001) can be discounted.*

In response to Item 1, Section C.I.2.4.6.1 of Regulatory Guide 1.206, and information provided in References 1 and 2, tsunami modeling was conducted for a submarine mass failure (SMF) originating at the East Breaks slump (Figure 1). A series of scaled dipolar initial conditions were used for bracketing possible minimum and maximum wave heights (References 3 and 4). Hydrodynamic simulations were modeled using a series of codes known as the Method of Splitting Tsunami (MOST) (References 5 and 6). For negative (i.e., drawdown) wave elevations of up to -140 m (-459 ft) and positive wave elevations of up to 60 m (197 ft), maximum predicted run-up along the South Texas coast did not exceed 2 m (6.6 ft) above Mean Sea Level (MSL).

The below discussion for Item 1 is separated into two sections. The first section discusses the geologic setting of the East Breaks slump. The second section discusses hydrodynamic simulations with MOST.

The East Breaks slump is located approximately 142 km (88 mi) to the southeast of STP 3 & 4 (Figure 1 and Figure 2). The coordinates of the slump are approximately 27.57 °N and 95.64 °W. The slump consists of an eastern lobe and a western lobe (Figure 3) (References 7 and 8). Reference 8 states that "the western and eastern lobes are thought to have formed by two

different processes, and actually at two different, but relatively close, time periods. The western lobe formed as a slump and debris deposits traveled downslope. The eastern lobe is more consistent with turbidity flow currents in the upper parts of the slide and leveed channels in the middle and lower portions of the slide." As turbidity flow currents are unlikely to have influenced tsunamigenesis (Reference 1, pp. 8-9), only the western lobe was used for the simulations.

The age of the East Breaks slump is not precisely known. Reference 7 states that the East Breaks landslide is dated from about 16,000 years before the present (hereinafter referred to as "ybp"). Reference 9 states that "the East Breaks Slide is a site of [sea level] lowstand instability, and seismic [reflection] data shows repeated slope failure in this area. During late Quaternary lowstands of sea level, large deltas built up along the Texas-Louisiana shelf margin, and the present continental shelf [became] exposed as a subaerial coastal plain." Reference 9 also stated that "it is clear that most sliding on the Texas-Louisiana slope occurred during the late Pleistocene lowstands of sea level when sedimentation rates on the upper slope were high."

Dimensions of the East Breaks slump scar have varied with different investigations. For example, Reference 2.4S.6-5 (i.e., Trabant et al., 2001) stated that the slump "consists of a 20-km wide head scarp initiated along the 150-meter isobath, a 55 km long erosional chute, ending in a 95x30 km accretionary lobe. Total extent of the feature is 160 km from the shelf edge to a depth of 1,500 m" and "slumped deposits extend over a 3,200-km^2 area with a volume on the order of 50-60 km^3." Reference 9 states that "the East Breaks Slide is a prominent mass-transport feature. Revised bathymetry shows that the slide originated on the upper slope (200-1000 m), in front of a sandy late Wisconsinan shelf-margin delta, where the gradient is up to 3°. It was deposited in a middle slope position (1000-1500 m) where the gradient is about 0.5°. Side-scan sonar data indicates that the slide is a strongly backscattering feature extending more than 110 km downslope from the shelf edge." Reference 1 states that "the largest of these failures occurs in the northwestern Gulf of Mexico, is 114 km long, 53 km wide, covers about 2,250 km^2, and has been interpreted to consist of at least two debris flows."

Source parameters for the East Breaks slump were estimated using three arc-second bathymetry data from the National Geophysical Data Center (NGDC) (Reference 11). Source parameters, including slump width, length, and thickness, were estimated using a Geographic Information Systems (GIS) environment (Figure 3). Slump width was estimated to be approximately 13.4 km. The length of the erosional chute was estimated to be about 42 km. Based on a transect across the erosional chute, slump thickness was estimated to be about 100 m (i.e., see Path Profile A to A' in Figure 3). With respect to slope, Reference 2.4S.6-5 (i.e., Trabant et al., 2001) stated that "initial failure of the slump took place on very low angle slopes of less than two degrees while present slump deposits have an average seafloor slope of one-degree." While a vertical drop of 850 m over a length of 42 km indicates a bed slope of approximately 1.1 degrees, a maximum local slope of 2 degrees was used from estimates in GIS as a conservative estimate. Similarly, initial depth of the slide was estimated conservatively using the 200-m and 1000-m bathymetry contour elevations. Therefore, initial depth was estimated to be 600 m (i.e., (200 m + 1000 m)/2) (Figure 1). The total length of the slide was estimated from Reference 1 as 114 km.

With respect to simulations, tsunami modeling was performed with MOST (References 5 and 6). Validation and verification of MOST is discussed in Reference 16 and Reference 2.4S.6-20. In brief, MOST is based on three phases of long wave evolution:

(i): A "Deformation Phase" that generates the initial conditions for a tsunami by simulating ocean floor changes due to a forcing mechanism;

(ii) A "Propagation Phase" that propagates the generated tsunami across the deep ocean using Nonlinear Shallow Water (NSW) wave equations; and

(iii) An "Inundation Phase" that simulates the shallow ocean behavior of a tsunami by extending the NSW calculations using a multi-grid "run-up" algorithm to predict coastal flooding and inundation.

Specification of an initial deformation condition was based on scaling a dipole wave (i.e., a wave with a dipolar structure). A dipole wave is similar to the structure of an N-wave (i.e., a tsunami with a leading negative or depression wave followed by a positive elevation wave). An initial dipole wave is characteristic of tsunamis from submarine landslides, and possibly all tsunamis (Reference 2.4S.6-20).

After specifying an initial deformation condition, the propagation phase is based on a simplified form of the Navier-Stokes equations referred to as the NSW equations in spherical coordinates (Eq. 1) (Reference 5):

$$h_t + \frac{(uh)_\lambda + (vh\cos\phi)_\phi}{R\cos\phi} = 0$$

$$u_t + \frac{uu_\lambda}{R\cos\phi} + \frac{vu_\phi}{R} + \frac{gh_\lambda}{R\cos\phi} = \frac{gd_\lambda}{R\cos\phi} + fv \qquad (1)$$

$$v_t + \frac{uv_\lambda}{R\cos\phi} + \frac{vv_\phi}{R} + \frac{gh_\phi}{R} = \frac{gd_\phi}{R} - fu$$

where λ is longitude; ϕ is latitude; $h = h(\lambda,\phi,t) + d(\lambda,\phi,t)$, $h(\lambda,\phi,t)$ is amplitude; t is time; $d(\lambda,\phi,t)$ is undisturbed water depth; $u(\lambda,\phi,t)$ and $v(\lambda,\phi,t)$ are depth-averaged velocities in longitude and latitude directions, respectively; g is gravitational acceleration; f is the Coriolis parameter ($f = 2\omega\sin\theta$); and R is the radius of the earth.

Eq. (1) is then solved numerically using a finite difference algorithm that splits the NSW equations into a pair of systems (Reference 6):

$$\left\{\begin{aligned} &h_t + (uh)_x = 0 \\ &u_t + uu_x + gh_x = gd_x \\ &v_t + uv_x = 0 \end{aligned}\right\} \text{ and } \left\{\begin{aligned} &h_t + (vh)_y = 0 \\ &u_t + vv_y + gh_y = gd_y \\ &v_t + vu_y = 0 \end{aligned}\right\} \qquad (2)$$

where x and y are coordinates corresponding to latitude and longitude in a Cartesian system, respectively. The two systems of equations are then solved sequentially at each time step. Additional details of the numerical solution of the MOST propagation are provided in Reference 2.4S.6-20 and Reference 6.

Since tsunami wavelength becomes shorter during shoaling, a series of nested grids are required for maintaining resolution of the wave with decreasing water depth. Therefore, three grids (i.e., A, B and C) were used for the MOST simulations (Figure 4). The grids were derived from NGDC topography and bathymetry data (Reference 11). Grid spacing between nodes was equal to 12 arc-seconds, 6 arc-seconds, and 6 arc-seconds, respectively.

MOST uses a moving boundary calculation for estimating tsunami run-up onto dry land. Details of the moving boundary are discussed in Reference 2.4S.6-20, Reference 6, and Reference 16. While friction factors are not used in the propagation phase of MOST, a Manning's roughness coefficient to the second power (n^2) must be specified for the inundation phase. Following sensitivity simulations, this value was set equal to 0.01 (i.e., n=0.1). This value was selected for maximizing stability throughout the duration of the simulations. Reference 6 also states that "several studies show that an unsteady flow during run-up is not very sensitive to changes in the roughness coefficient...any moving boundary computation induces numerical friction near the tip of the climbing wave (except in a Lagrangian formulation)."

Initial wave dimensions were estimated using the slump center of mass motion model described in Reference 17 and Reference 18. Source parameters documented in the paragraphs above and in Figure 3 were used for estimating the initial drawdown due to a depression wave from the landslide. Specific gravity of the slump mass was assumed to be equal to 2. The 100-m thickness (T) of the East Breaks slump with respect to the 600-m initial depth (h) (T/h=0.17) and the slump thickness relative to the 42 km length (b) of the erosional chute (T/b=0.002) suggests the initial wave height from the East Breaks slump would be relatively small. Using the NGDC bathymetry data (Figure 3) and References 17 and 18, initial wave height for the East Breaks slump was estimated to be 7.9 m. Considering variability in interpreting landslide dimensions, the estimate of 7.9 m is similar to the "tsunami wave on the order of 7.6 meters" predicted by Trabant et al. (2001) [Reference 2.4S.6-5].

As noted in the preceding paragraphs, interpretation of slump dimensions can vary considerably (Reference 14). Therefore, estimates of initial conditions (i.e., wave height and shape) are not easily replicable between investigators. Consequently, scaling initial wave height into a dipole wave condition was based on deformations from other landslide tsunami investigations (Reference 12). A similar approach was used in Reference 3 and Reference 4.

Initial deformation conditions of the water surface included the Palos Verdes (PV) landslide in Southern California (Reference 4), the Palos Verdes wave scaled by twenty times (PVx20), the 1998 Papua New Guinea (PNG) slump in the Sandaun Province (Reference 12), and a hypothetical "Monster" wave condition. Scaled initial conditions were used for the simulations as relatively little data exists for landslide tsunamis, and the PV and PNG events have been tested extensively by the tsunami community (Reference 4 and Reference 2.4S.6-20). The hypothetical "Monster" case has not been previously tested by the tsunami community. The

hypothetical "Monster" case was developed as a complementary case for the East Breaks slump to test a very wide initial wave, as opposed to a tall and steep initial wave.

Minimum and maximum elevations for the initial deformation cases are listed in Table 1. Initial conditions were based on a scaled dipole wave located at the centroid of the East Breaks slump. All cases were oriented relative to the slump. Minimum (negative) and maximum (positive) elevations for each case were as follows:

1. Palos Verdes (PV): -7 m (-23 ft) and 3 m (10 ft) (Figure 5 and Figure 6);
2. Palos Verdes scaled by twenty times (PVx20): -140 m (-459 ft) and 60 m (197 ft) (Figure 7 and Figure 8);
3. Papua New Guinea (PNG): -20 m (-66 ft) and 16 m (53 ft) (Figure 9 and Figure 10); and
4. Hypothetical "Monster" (Monster): -38 m (-125 ft) and 27 m (89 ft) (Figure 11 and Figure 12).

Table 1. Initial wave deformation characteristics for simulations and corresponding maximum run-up along the South Texas Coast near STP 3 & 4.

Case	Dipole Initial Minimum (m below MSL)	Dipole Initial Maximum (m above MSL)	Maximum Run-up (m above MSL)
PV	-7	3	1
PV(x20)	-140	60	2
PNG	-20	16	2
Monster	-38	27	2

MOST output includes run-up estimates (i.e., maximum inland elevation inundated by the tsunami above MSL). Maximum run-up ranges from 1 to 2 m (3.3-6.6 ft) (MSL) for the South Texas coast near STP 3 & 4 (Table 1). Plots of maximum wave amplitude relative to South Texas coast bathymetry are shown for PV, PV(x20), PNG, and the hypothetical "Monster" cases in Figure 13, Figure 15, Figure 17, and Figure 19, respectively. Time series and period of water surface elevation above MSL for a buoy location near the South Texas coast for the PV, PV(x20), PNG, and hypothetical "Monster" are shown in Figure 14, Figure 16, Figure 18, and Figure 20, respectively.

Nuclear regulatory requirements for the PMT analysis do not explicitly require an analysis of the 10% exceedance of the astronomical high tide or long-term sea level rise as a combined event with the PMT. However, for this assessment, the maximum flood level for a PMT event includes the 10% exceedance of the astronomical high tide and long-term sea level rise. As regulatory criteria for these components are only available for the Probable Maximum Storm Surge (PMSS), the criteria for the PMSS in Regulatory Guide 1.59 (1977) and ANSI 2.8 (1992) were adopted for the PMT analysis. Based on tide gauge data for NOS Station #8772440 ("Freeport, Texas"), the 10% exceedance of the astronomical high tide was estimated to be 1.08 m (3.54 ft) NGVD29 (or MSL). The long-term sea level rise for this station was estimated by NOAA to be 4.35 mm/year or 0.44 m (1.43 ft) per century. The peak flood level due to a

probable maximum tsunami event is therefore estimated to be on the order of 3.52 m (11.5 ft) MSL within the next century (i.e., 3 m (MSL) tsunami run-up + 1.08 m (MSL) 10% exceedance of the astronomical high tide + 0.44 m (MSL) sea-level rise = 3.52 m).

A tsunami run-up of 11.5 ft MSL is below the design basis flood level of 48.5 ft (MSL) from the postulated Main Cooling Reservoir (MCR) breach (Subsection 2.4S.4 of COLA Rev 2). It is therefore not the controlling event for the design basis flood determination for STP 3 & 4 safety-related structures.

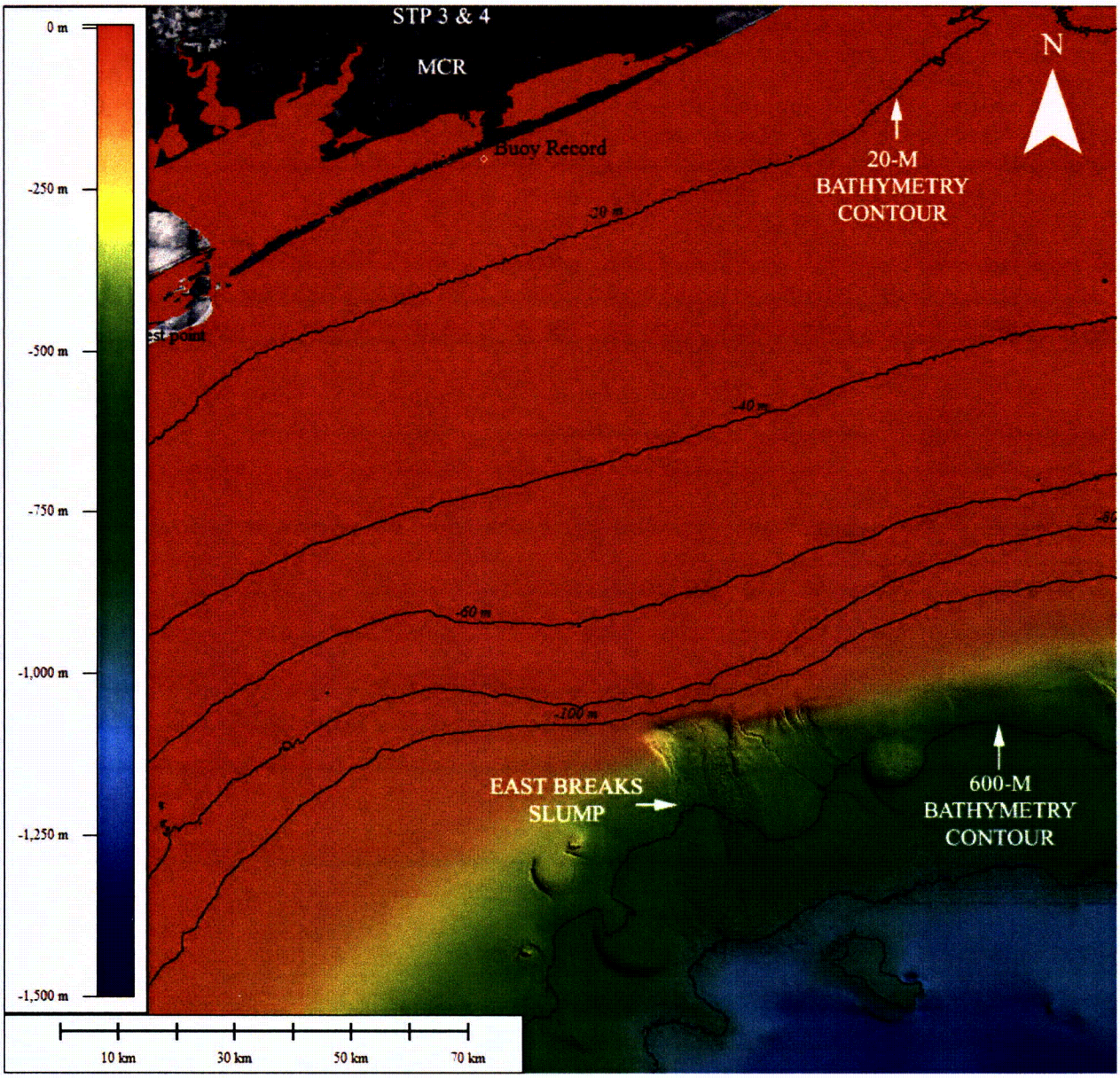

Figure 1. Location of East Breaks slump relative to STP 3 & 4 (Source: Reference 11). Bathymetry elevations are relative to Mean Sea Level (MSL).

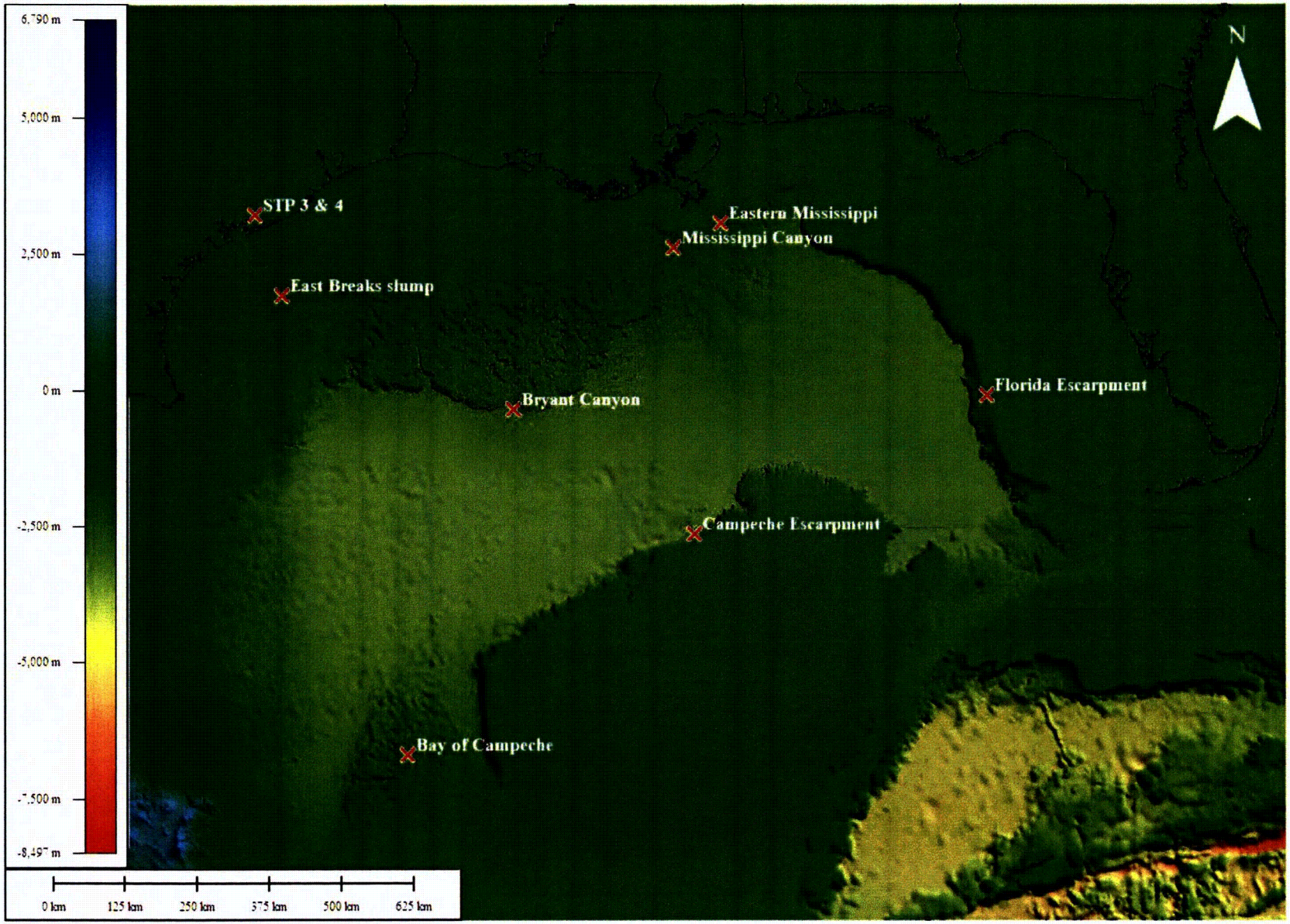

Figure 2. SMF regions in Gulf of Mexico. At 142 km from STP 3 & 4, the East Breaks slump is the only near-field landslide source. Datum is relative to MSL. Source of bathymetry: Reference 11. Source of SMF locations: Reference 10.

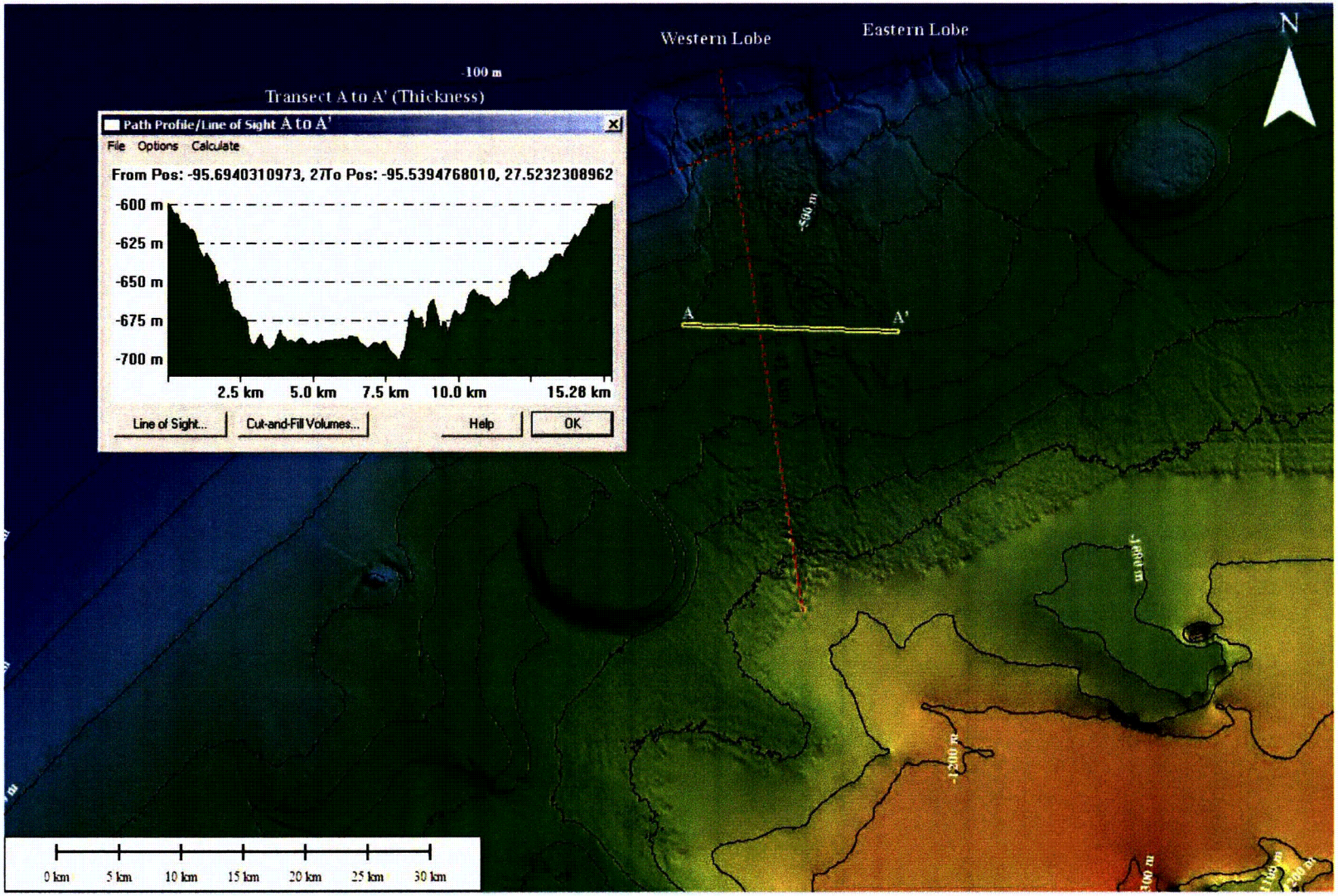

Figure 3. Source parameters for East Breaks slump (Source: Reference 11). Bathymetry elevations are relative to MSL.

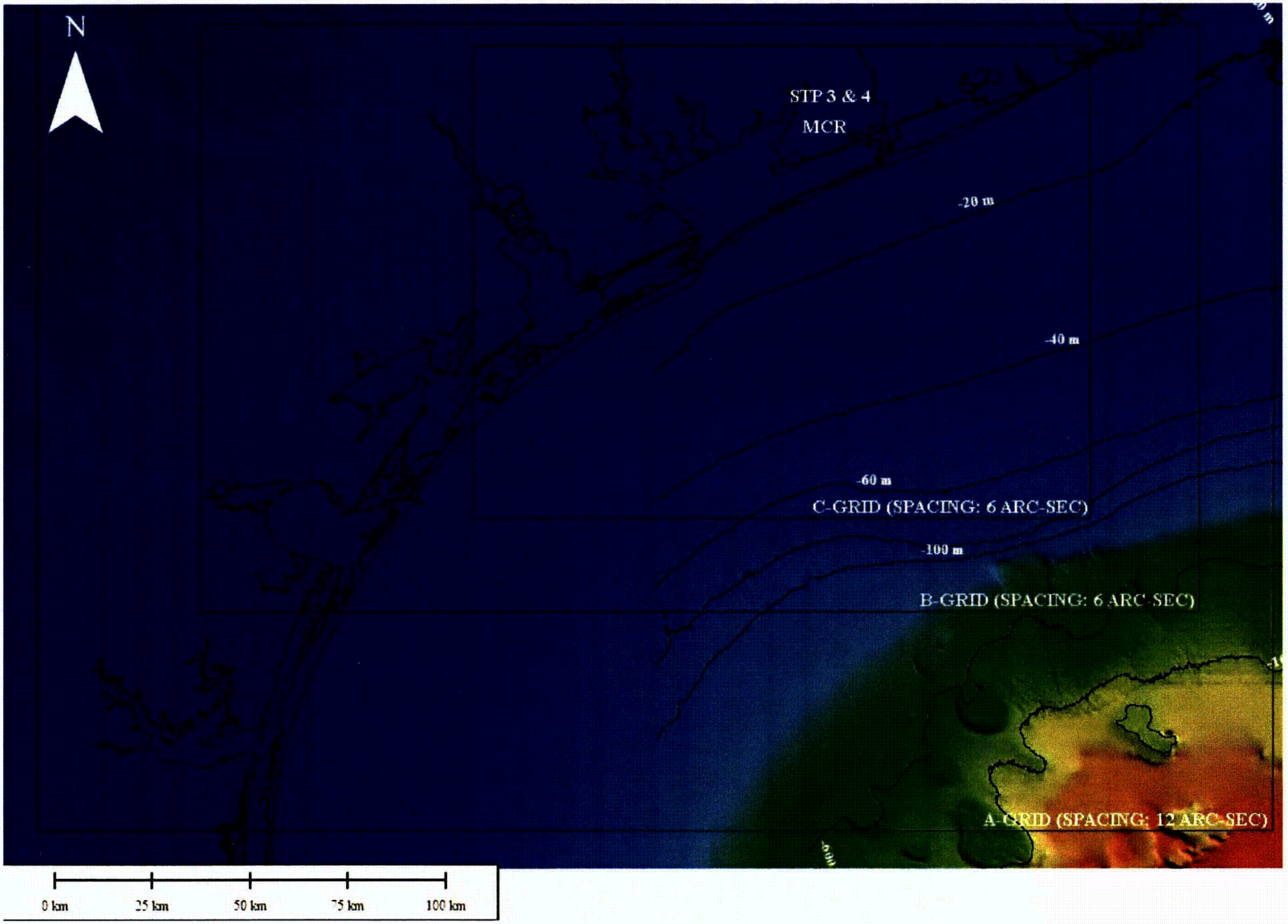

Figure 4. Grid spacing for East Breaks slump modeling with MOST (Source of bathymetry data: Reference 11). Bathymetry elevations are relative to MSL.

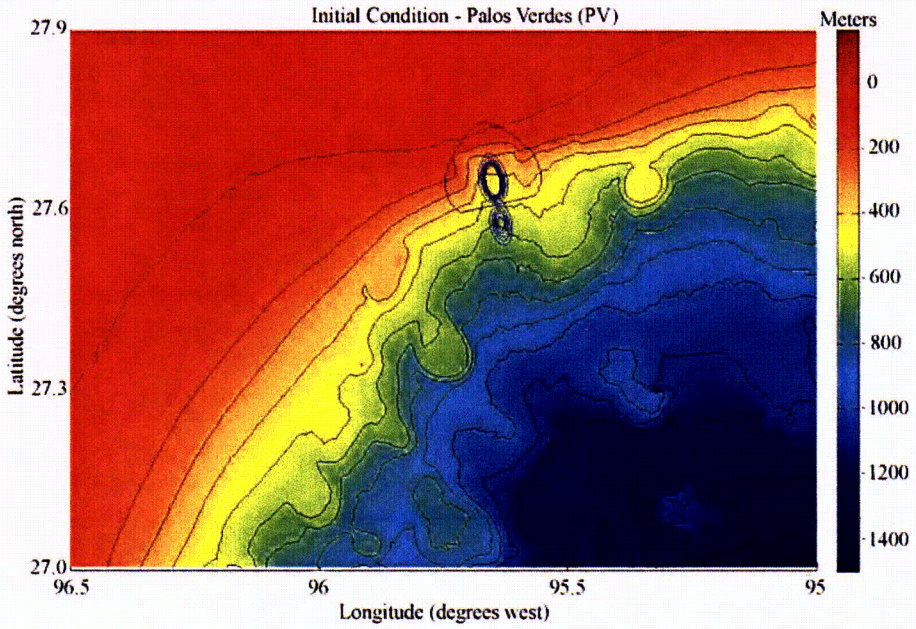

Figure 5. Plan view of Palos Verdes (PV) initial condition showing 2-D deformation at the East Breaks slump location. Elevations of contour lines correspond with elevations in Figure 6.

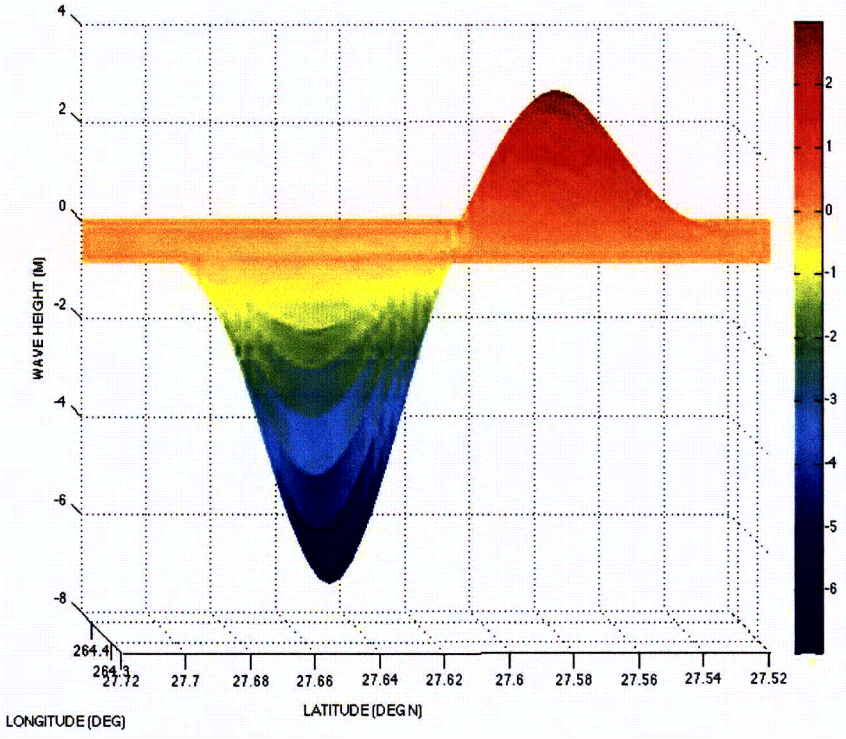

Figure 6. Side view of Palos Verdes (PV) initial deformation condition.

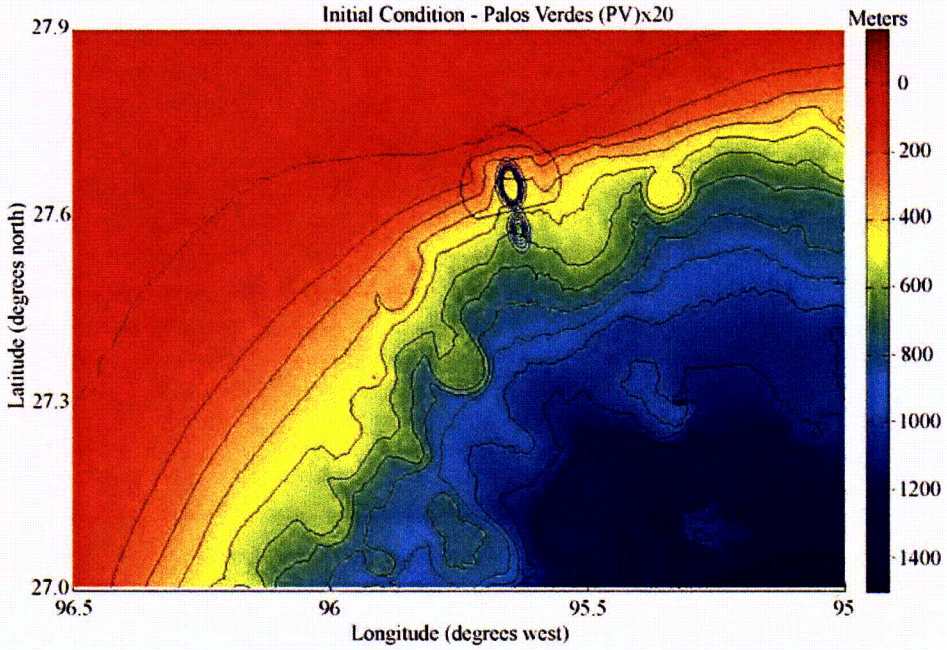

Figure 7. Plan view of Palos Verdes x20 (PVx20) initial condition showing 2-D deformation at the East Breaks slump location. Elevations of contour lines correspond with elevations in Figure 8.

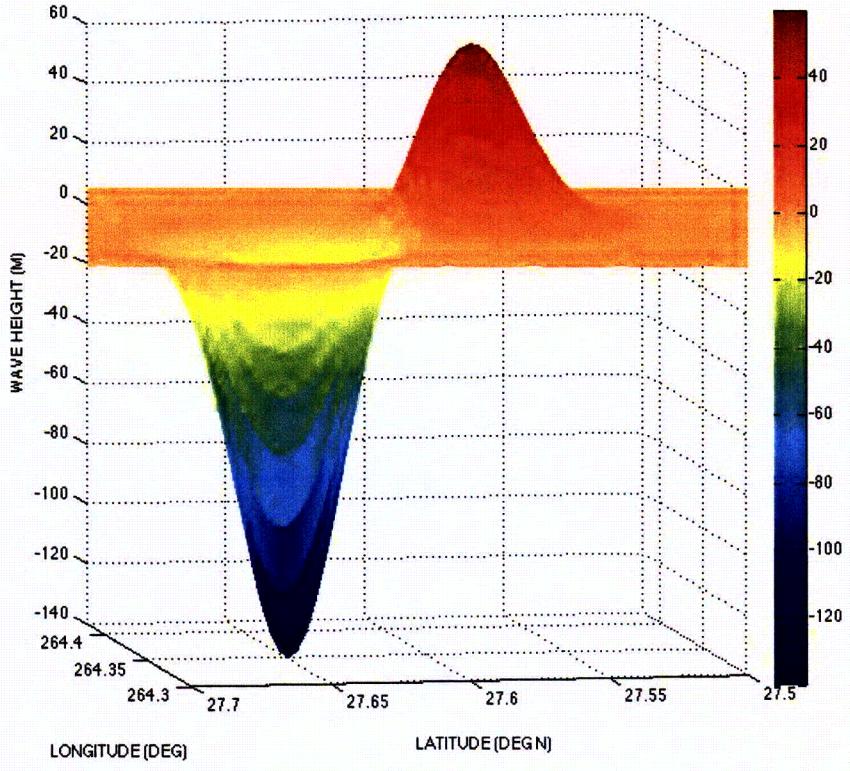

Figure 8. Side view of Palos Verdes x20 (PVx20) initial deformation condition.

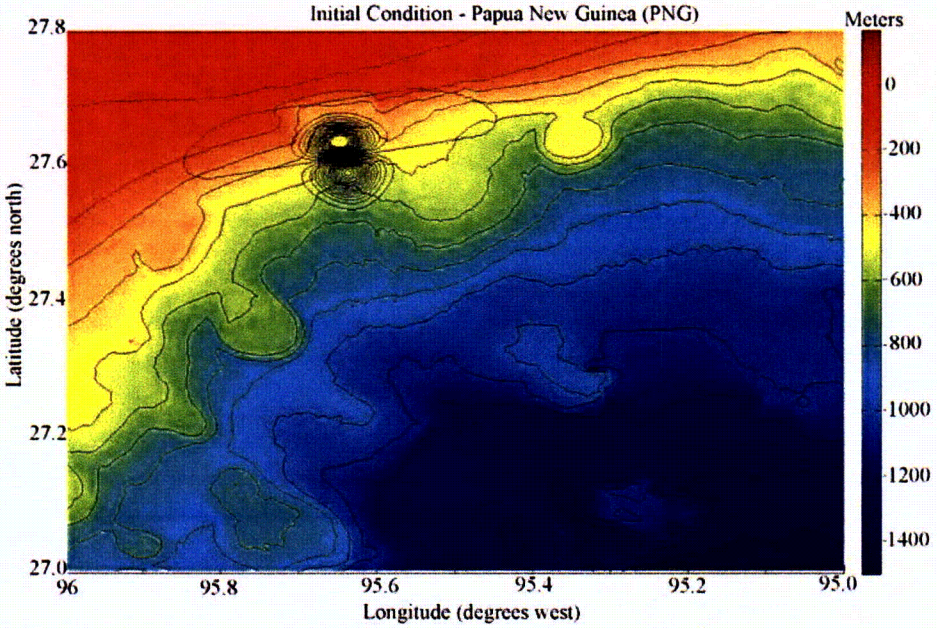

Figure 9. Plan view of Papua New Guinea (PNG) initial deformation condition at the East Breaks slump location. Elevations of contour lines correspond with elevations in Figure 10.

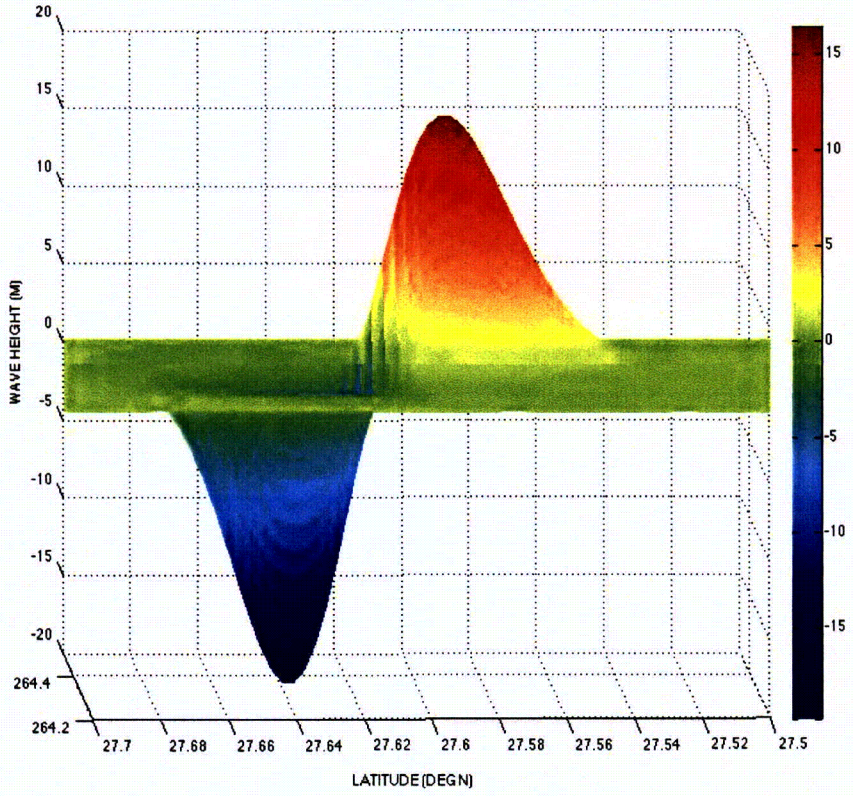

Figure 10. Side view of Papua New Guinea (PNG) initial deformation condition.

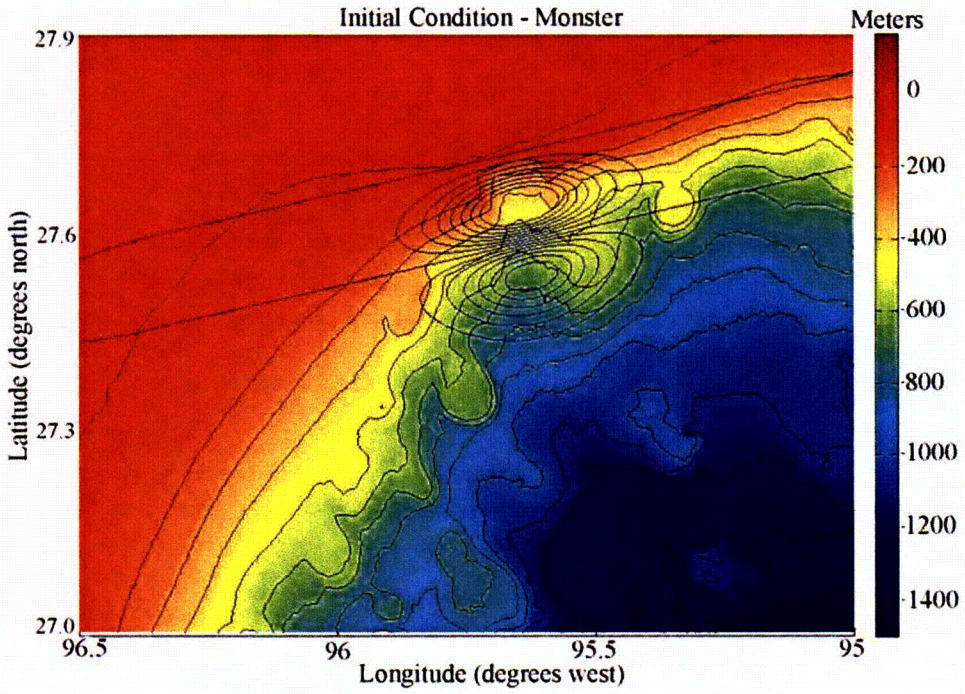

Figure 11. Plan view of hypothetical "Monster" initial condition showing 2-D deformation at the East Breaks slump location. Elevations of contour lines correspond with elevations in Figure 12.

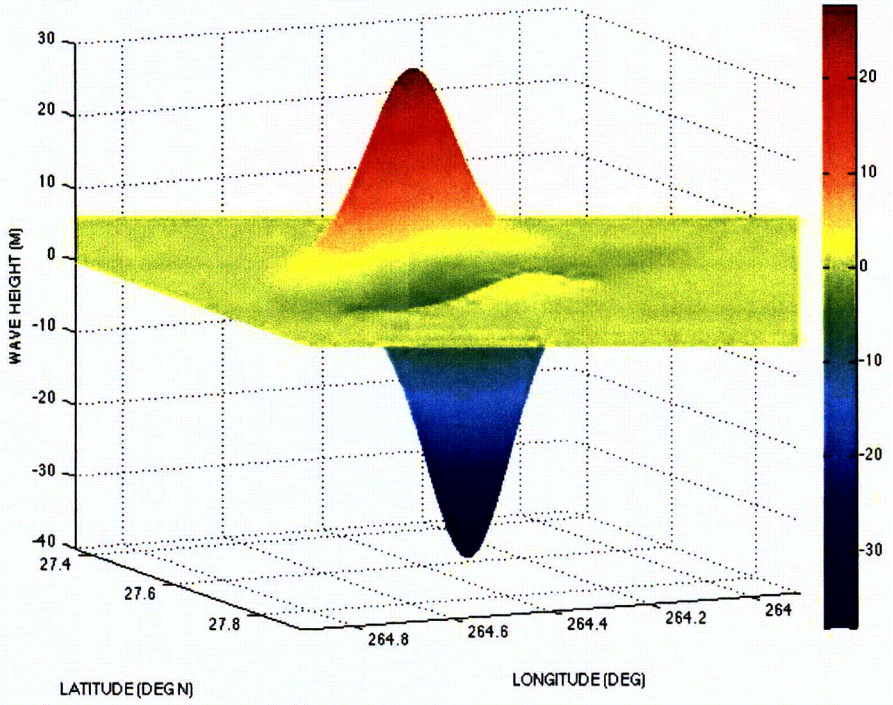

Figure 12. Oblique view of hypothetical "Monster" initial deformation condition.

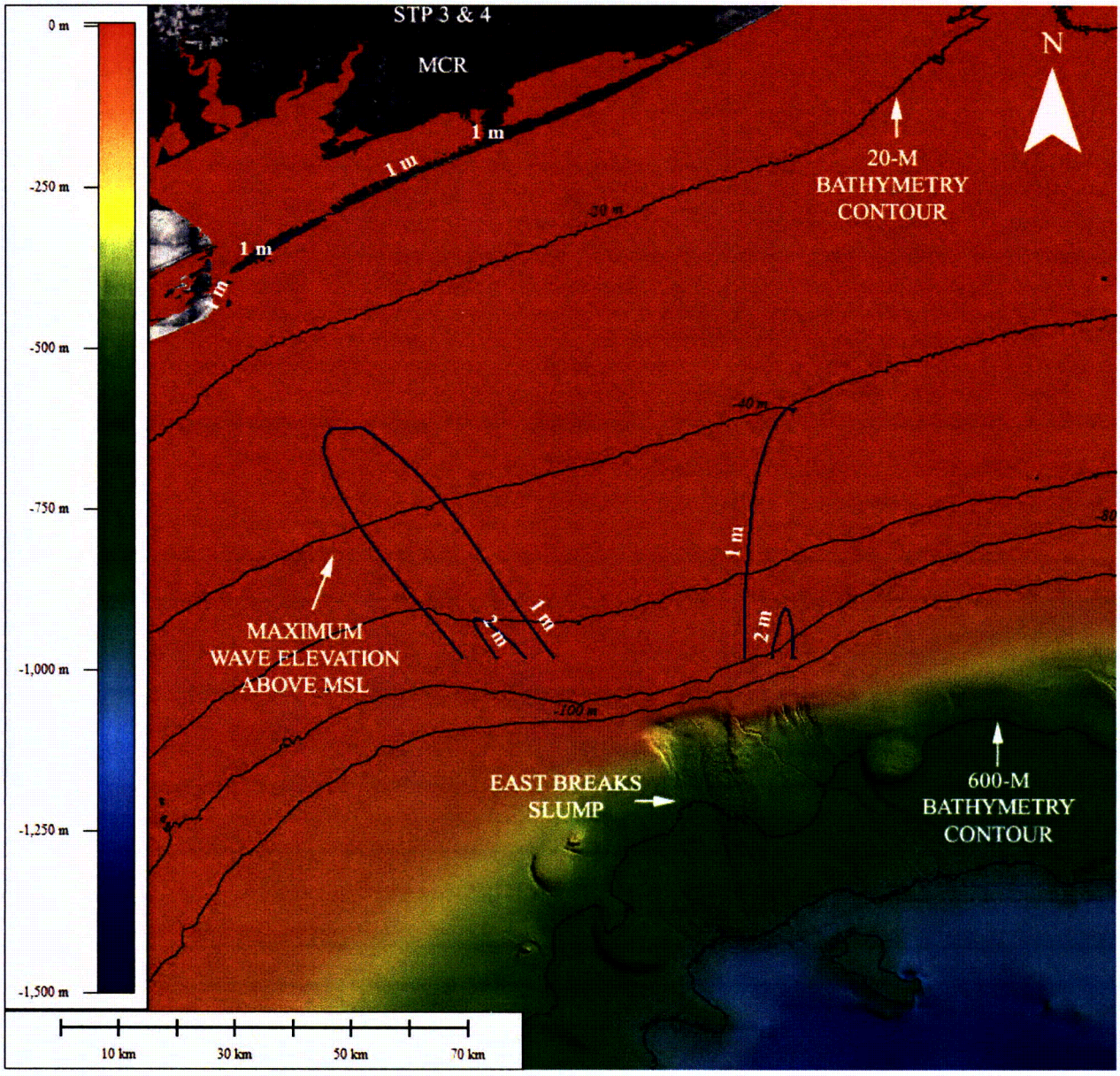

Figure 13. Maximum coastal run-up for the PV case was 1 m.

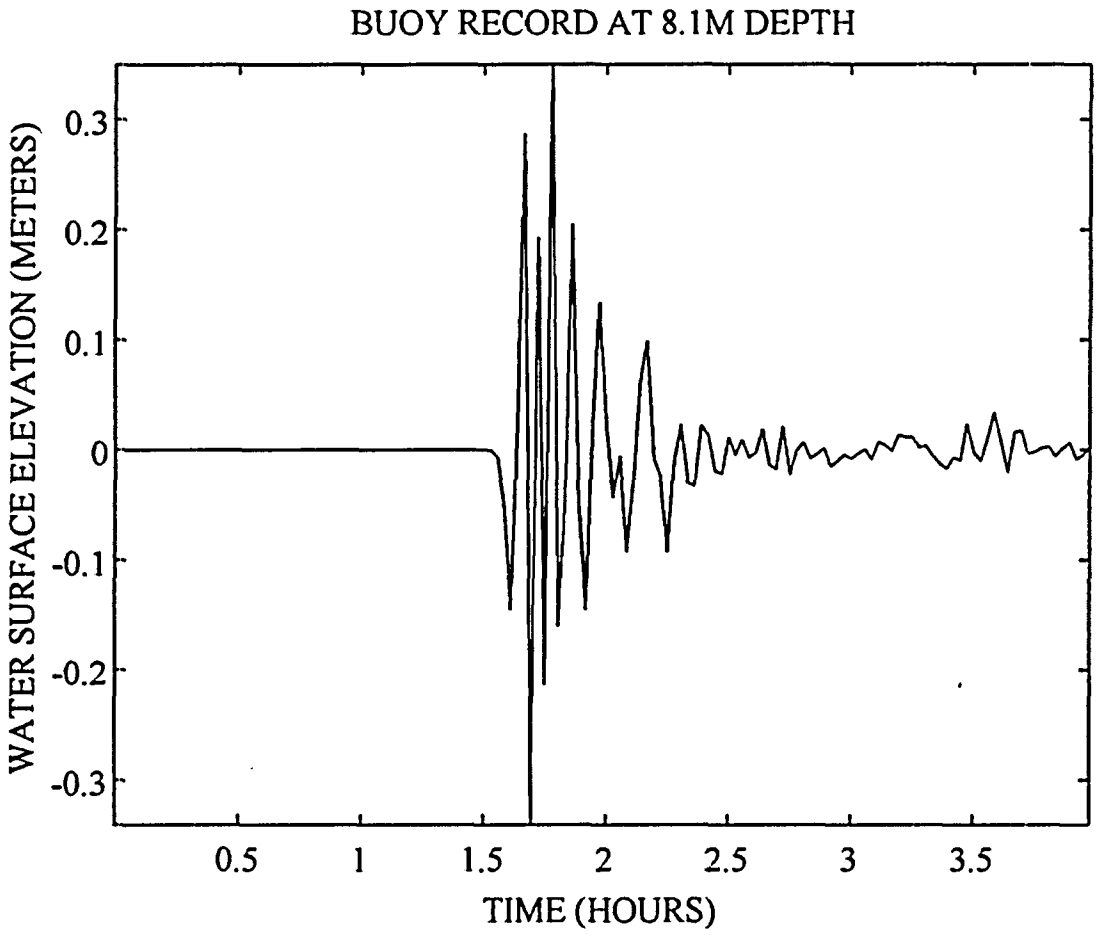

Figure 14. Time series of PV water surface elevation at 28.58 deg N and 95.98 deg W (i.e., buoy location shown in Figure 1). Datum referenced to MSL.

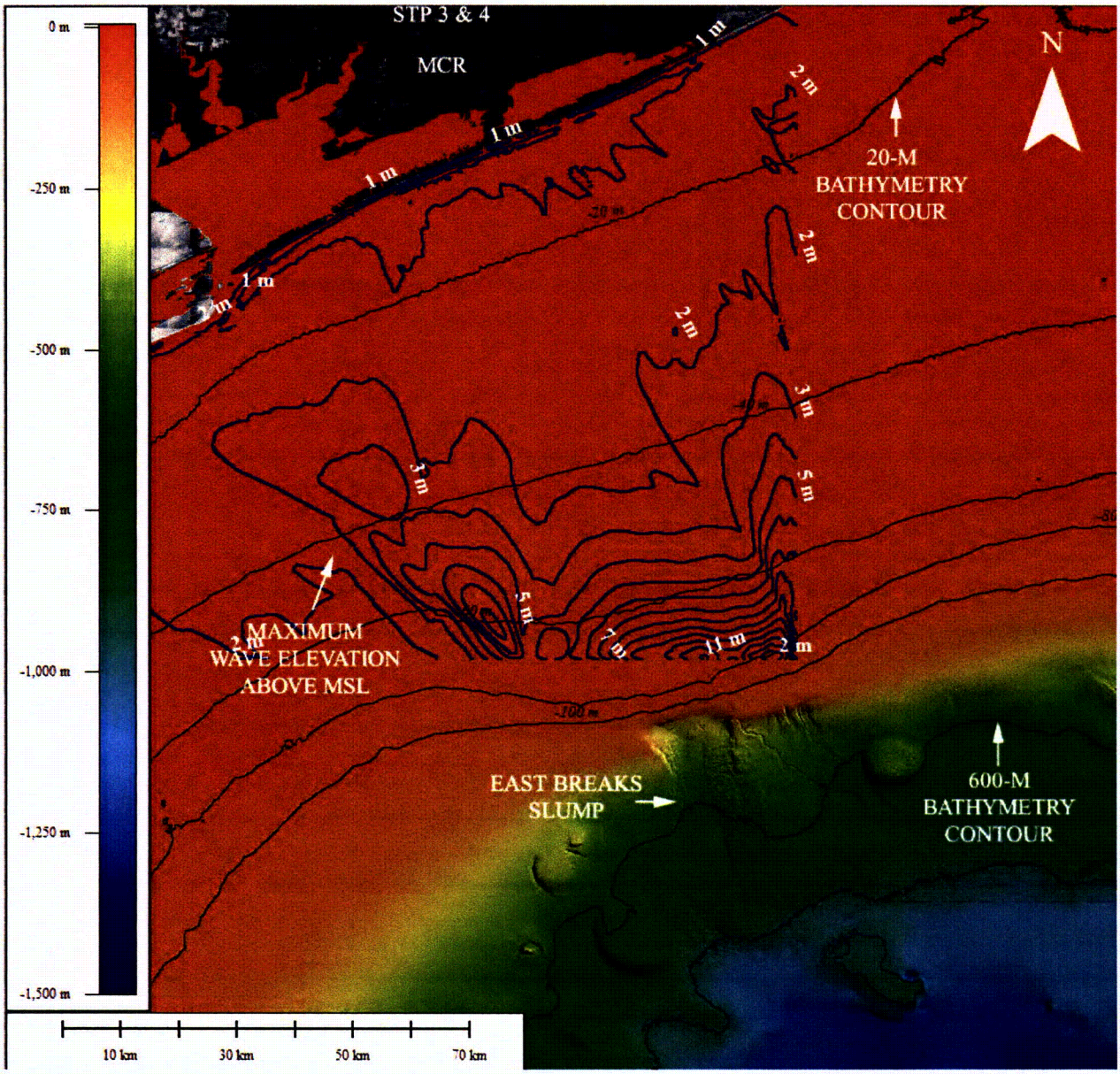

Figure 15. Maximum coastal run-up for the PV(x20) case was 2 m.

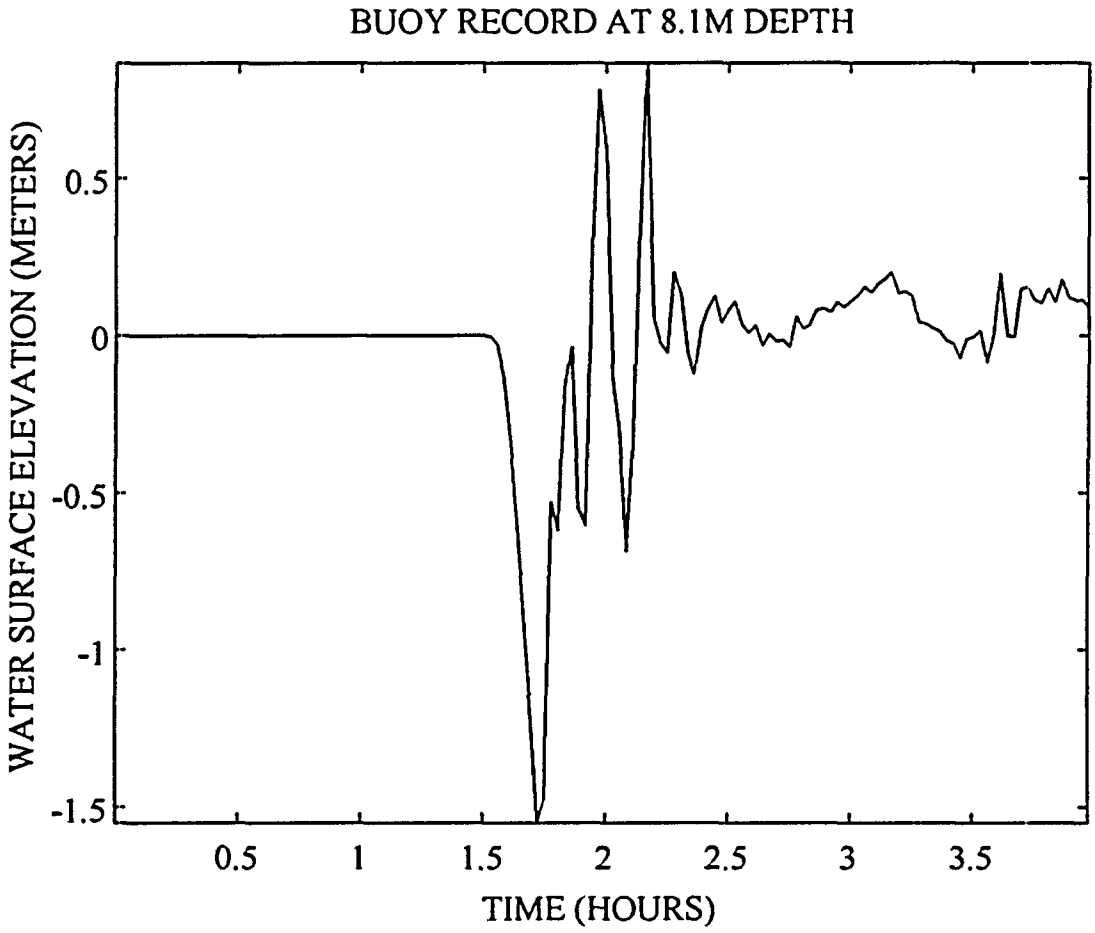

Figure 16. Time series of PV(x20) water surface elevation at 28.58 deg N and 95.98 deg W (i.e., buoy location shown in Figure 1). Datum referenced to MSL.

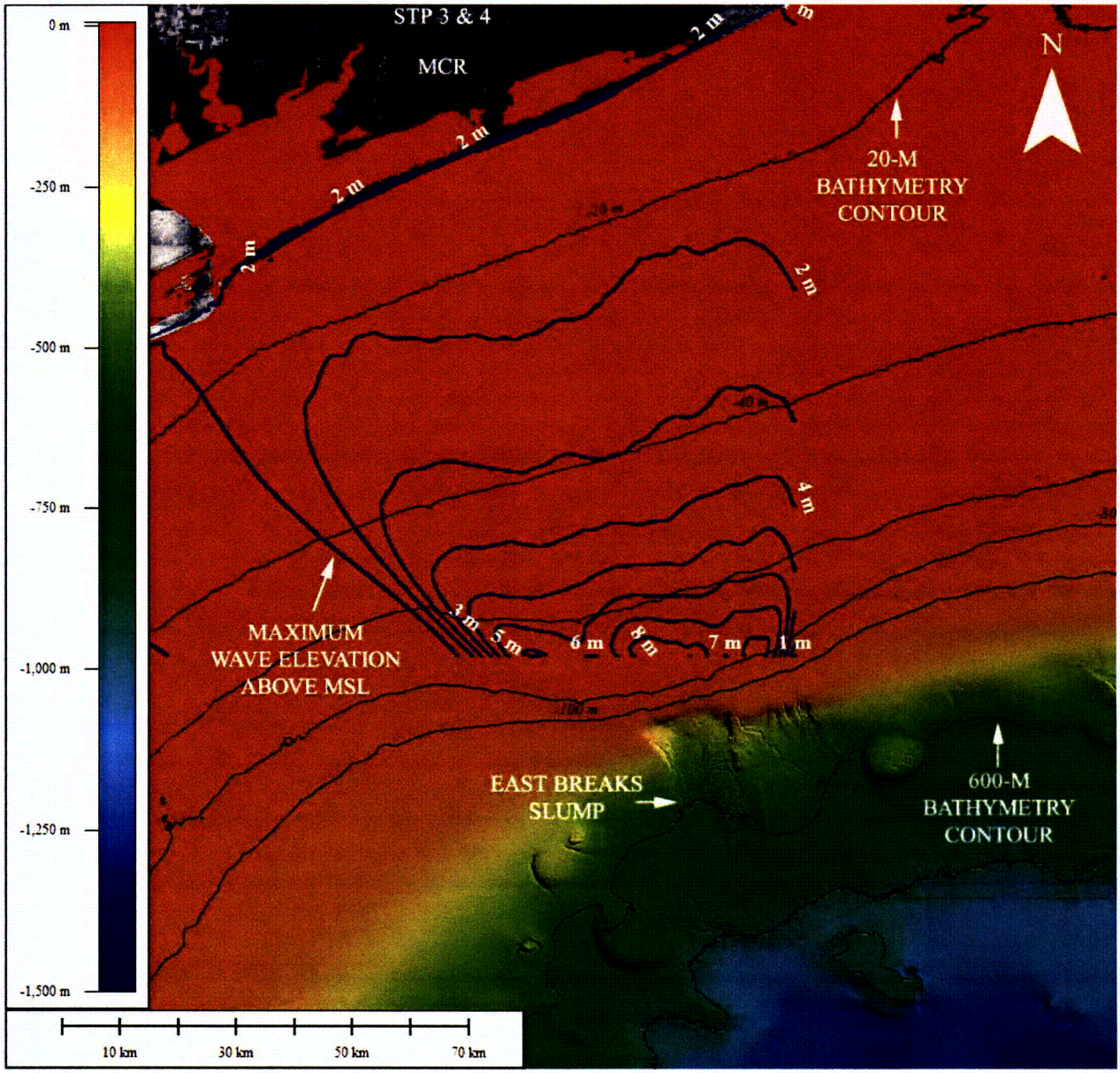

Figure 17. Maximum coastal run-up for the PNG case was 2 m.

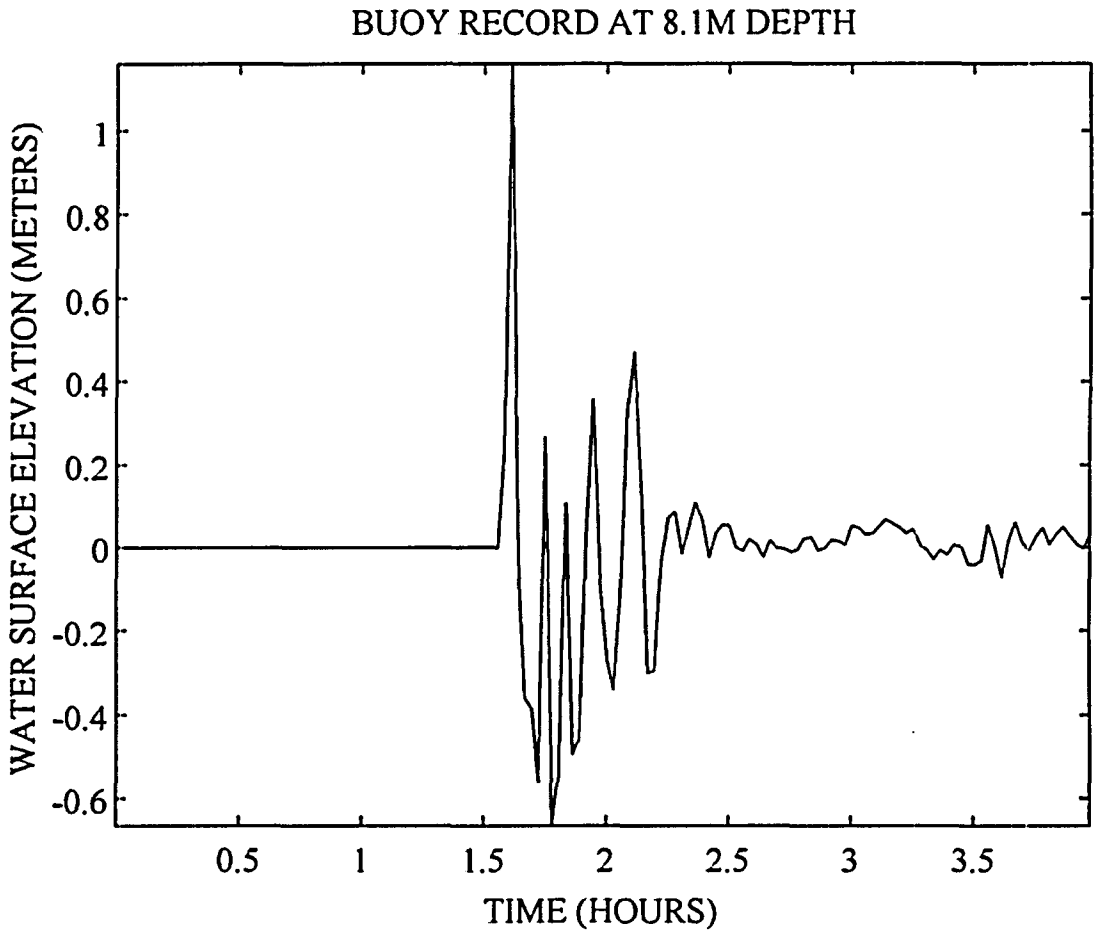

Figure 18. Time series of PNG water surface elevation at 28.58 deg N and 95.98 deg W (i.e., buoy location shown in Figure 1). Datum referenced to MSL.

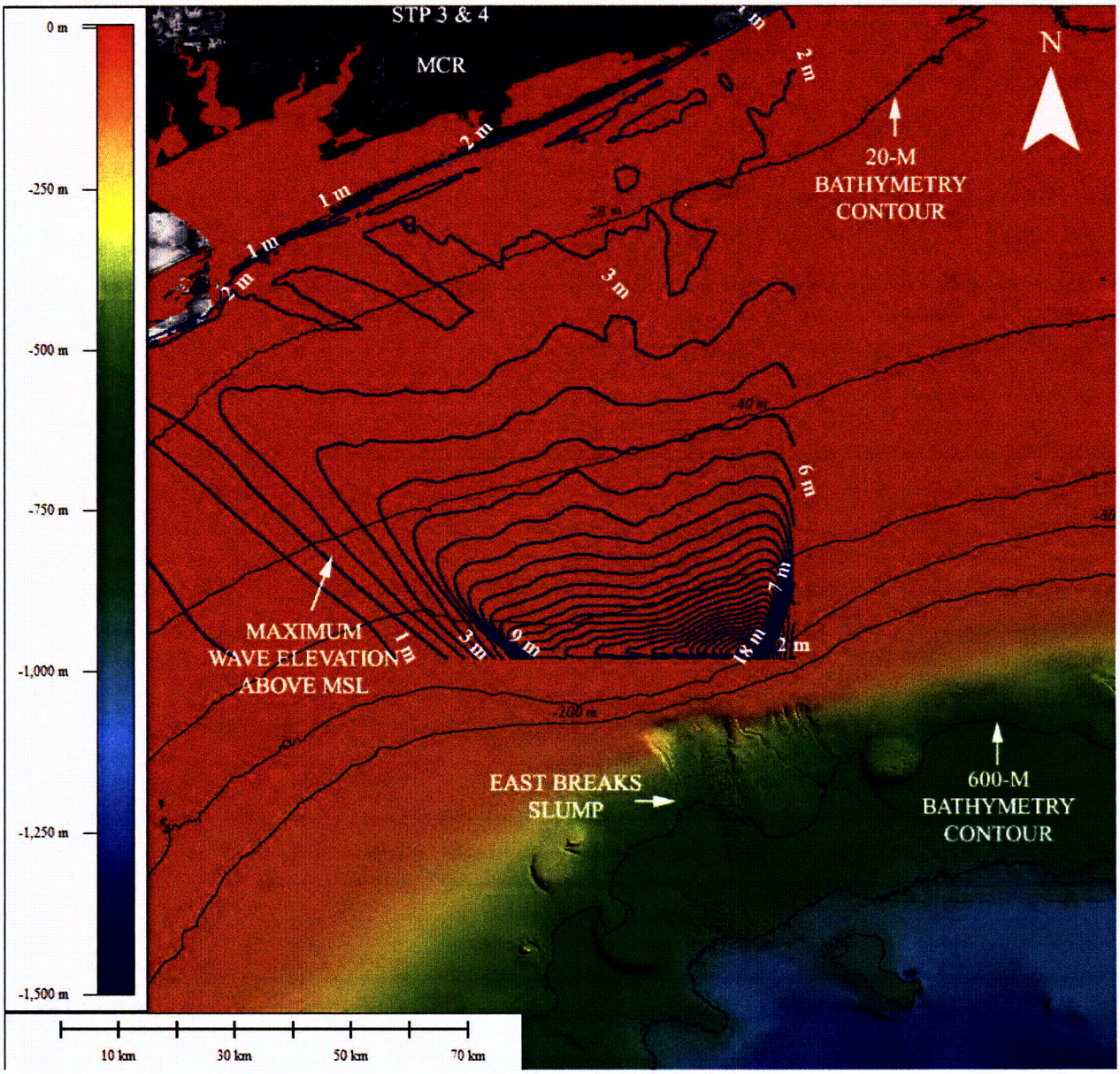

Figure 19. Maximum coastal run-up for the hypothetical "Monster" case was 2 m.

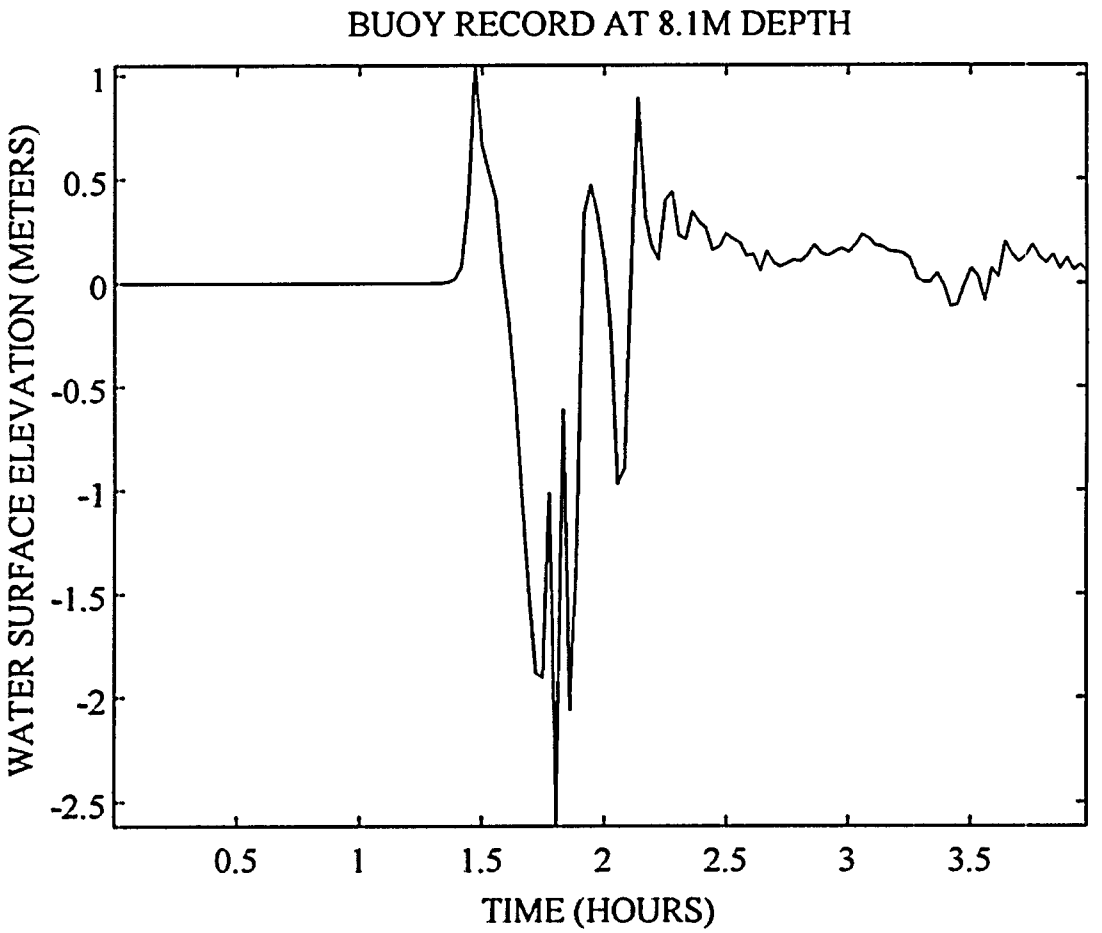

Figure 20. Time series of hypothetical "Monster" water surface elevation above MSL at 28.58 deg N and 95.98 deg W (i.e., buoy location shown in Figure 1). Datum referenced to MSL

[Item 2] *In addition, provide an assessment of other regions in the Gulf of Mexico prone to landslides.*

In response to Item 2, Reference 1 (p. 35) cites four credible SMF source areas in the Gulf of Mexico (Figure 2), the Northwest Gulf of Mexico, Mississippi Canyon, Florida Escarpment, and Campeche Escarpment. These four SMF source areas are located in three geologic provinces: a carbonate province, a salt province, and a canyon to deep-sea fan province. The postulated SMF sources in the carbonate province are located offshore of West Florida and in the Campeche Escarpments north of the Yucatan Peninsula. The largest scar in this region is along the central part of the West Florida Slope and is estimated as 120 km long, 30 km wide, with a total volume of material removed of about 1,000 km^3. However, the formation of the scar was believed to have occurred as a result of multiple events. Most of the sediment was believed to have been removed before the middle of the Miocene [c. 11.6 million years ago]. The salt province is located in the northwestern Gulf of Mexico. The largest documented SMF in the salt province is

the East Breaks slump, which is discussed in the preceding paragraphs. Lastly, three canyon/fan systems are present in the canyon to deep-sea fan province: the Bryant, the Mississippi, and the Eastern Mississippi systems (Reference 10). These fan systems were formed during the Pliocene and Pleistocene. The Mississippi Fan is the largest of the three fans, though Reference 1 states that the resumption of hemipelagic sedimentation in the head of the Mississippi Canyon by 7500 ybp indicates that the largest of the landslide complexes ceased being active by the middle of the Holocene. The largest landslide in the complex covers approximately 23,000 km^2 and reaches 100 m in thickness, with a volume estimated to be on the order of 1,725 km^3. Geologic Long-Range Inclined Asdic (GLORIA) imagery suggests that this feature consists of at least two separate events (Reference 1).

The initial deformation conditions listed in Table 1 plausibly exceed wave heights from propagating tsunamis that may occur due to landslides in remote areas of the Gulf of Mexico. For example, relative to the location of STP 3 & 4, most SMF sources in the Gulf of Mexico are mid-field to far-field sources (Figure 2). The distance from STP 3 & 4 to the East Breaks slump is 142 km (88.2 mi). The distance from STP 3 & 4 to Bryant Canyon is 517 km (321.2 mi). The distance from STP 3 & 4 to Mississippi Canyon and the Eastern Mississippi Canyon/Fan is 640 km (397.7 mi) and 709 km (440.6 mi), respectively. The distance from STP 3 & 4 to the Campeche Escarpment and Bay of Campeche is 873 km (542.5 mi) and 953 km (592.2 mi), respectively. The distance from STP 3 & 4 to the Florida escarpment is 1169 km (726.4 mi). Since landslide waves are steep (i.e., high initial wave height relative to wavelength) and prone to breaking, wave heights at the East Breaks slump from mid-field and far-field sources (i.e., exceeding a distance of 200 km) as shown in Figure 2 are not expected to exceed the scenarios modeled in the MOST simulations. Further, as shown in the simulations, diffusion and energy dissipation of the waves generated from SMFs can be significant. Therefore, potential run-up from these events is expected to be lower than the modeled scenarios for the East Breaks slump, and additional landslide scenarios in the Gulf of Mexico are not further considered.

[Item 3] *To independently validate whether no tsunami hazard exists for the proposed site, provide geologic methods and tsunami identification criteria used to justify the determination that no tsunami deposit was found at the site.*

In response to Item 3, the geologic setting of the East Breaks slump is described in Subsection 2.4S.9 and Item 1. The slump itself was formed in late Wisconsinan delta sediments that are hypothesized to have originated from ancestral Colorado and Brazos River systems (References 7, 9, and 10). Reference 9 states that the failure of the East Breaks slump occurred "during the late Wisconsinan [i.e., 10,000 to 29,000 years before present] lowstand of sealevel," and that "the prograding deltaic foreset beds, overlying transgressive shale, overloaded the shelf edge, causing failure. Therefore, it seems likely that the East Breaks Slide is related to the deposition of Delta A [i.e., the delta formed from the ancestral Colorado and Brazos River systems]. The slide probably represents a single large-scale sediment failure." Further, "low rates of deposition may be a primary reason for the present stability over much of the upper slope, and a further indication that sediments are relatively stable." With the forcing mechanism for the slump failure stabilized by a relatively high present-day sea level and sediment loading limited by

major dams in the Colorado River (Subsections 2.4S.1 and 2.4S.9), the forcing mechanism for the East Breaks slump is not considered to be active.

Geologic criteria for the identification of tsunami deposits are discussed in Reference 16. As noted in Reference 16, a "combination of both the facies and sedimentology [approaches] has resulted in an often-used, if not universally approved, set of criteria for understanding how sandy tsunami deposits might be distinguished in the stratigraphic record." These criteria include sand layers that are less than 25 cm thick and laterally continuous for hundreds of meters; a generally landward thinning sand sheet; an isochronous sand layer that typically cuts across stratigraphy; sands that contain a heterogeneous collection of marine microfossils; sands that are massive or plane laminated; evidence of erosion; decreasing grain size landward and upward, with possible inverse grading; and relative abundance of marine geochemical tracers such as bromine.

The distance from the location of the East Breaks slump to STP 3 & 4 is approximately 142 km (88 mi). As the area spanning this distance was likely to have included inorganic (e.g., sands, pebbles, gravels) and organic (e.g., large trees) material, geologic evidence for a tsunami, if present, would likely be composed of materials discussed in the preceding paragraph. As discussed in Items 2 and 5, and the following paragraph, no evidence of this type has been found. The proximity of the site with respect to a probable window of run-up is discussed further in Item 5.

The presence of sand at STP 1 & 2 is indicative of a historical low-energy overbank floodplain adjacent to a meandering and avulsion-based deltaic river system (STP 3 & 4 FSAR References 2.4S.9-12 and 2.4S.9-13). As discussed in Subsection 2.4S.9, the path of the Lower Colorado River and nearby Texas rivers has been subject to major historical avulsions commensurate with long-term fluctuations in sea level. Geologically, avulsion and flooding of these systems contributed directly to sediment deposition observed near the proposed site for STP 3 & 4. Geomorphic processes in the site region and vicinity are described in Subsection 2.5S.1. Fluvial deposits of the late Pleistocene Beaumont Formation are mapped within the 25-mile site vicinity on Figure 2.5S.1-14. Geologic reconnaissance and mapping in the 5-mile radius site area and 0.6-mile radius site document the presence of Late Pleistocene Beaumont Formation facies, recent alluvium, historic dredged materials and fill (Figures 2.5S1-27 & 1-28). The natural deposits of the Beaumont Formation are consistent with detailed mapping investigations in Matagorda County (Reference 2.5S.1-38).

[Item 4] *Provide excavation photos from Units 1 and 2.*

In response to Item 4, excavation photos are provided in Figure 21, Figure 22, and Figure 23. The excavation photos do not reveal any evidence of a tsunami at the location of the MCR or at STP 1 & 2.

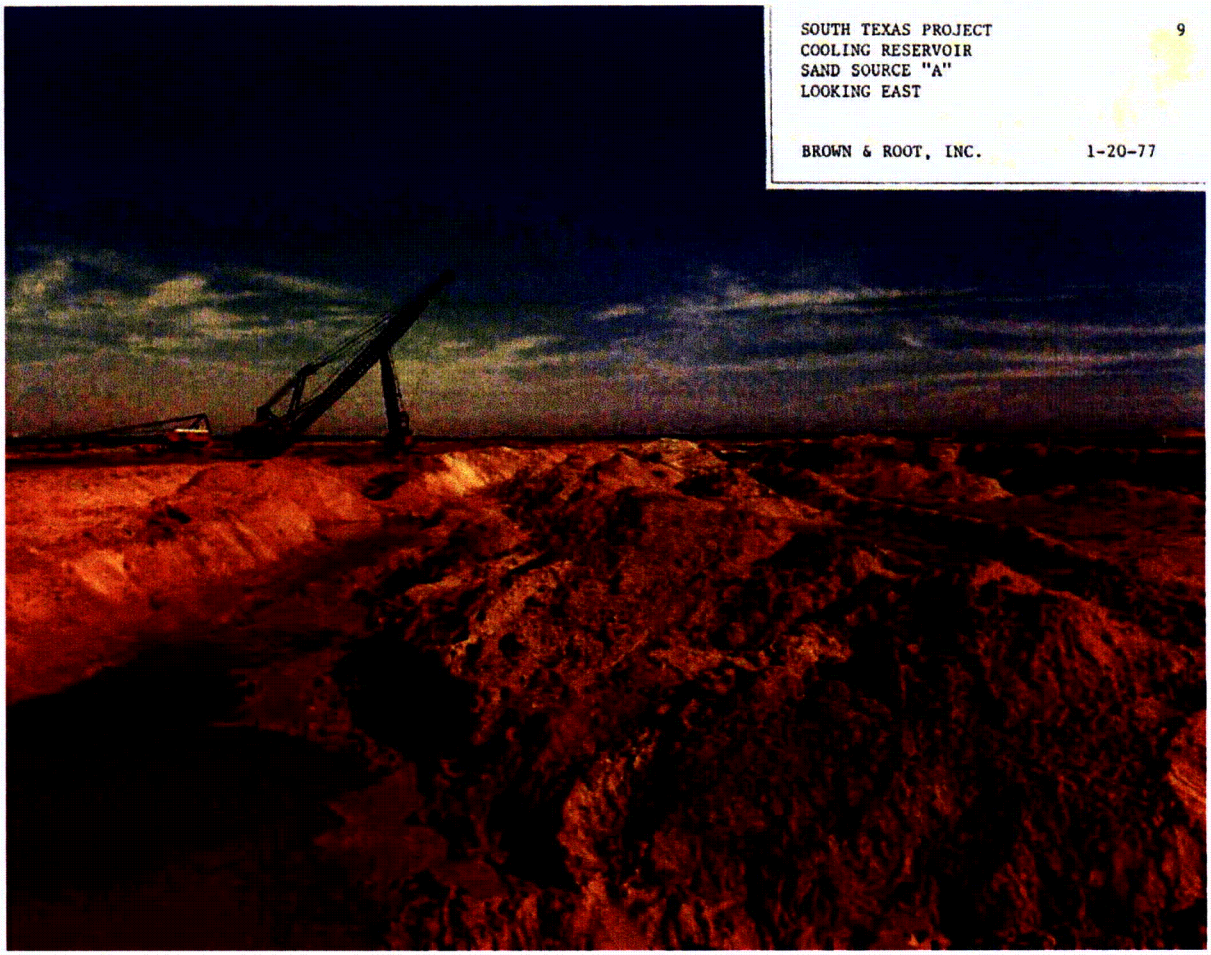

Figure 21. Sands in the MCR near STP 3 & 4.

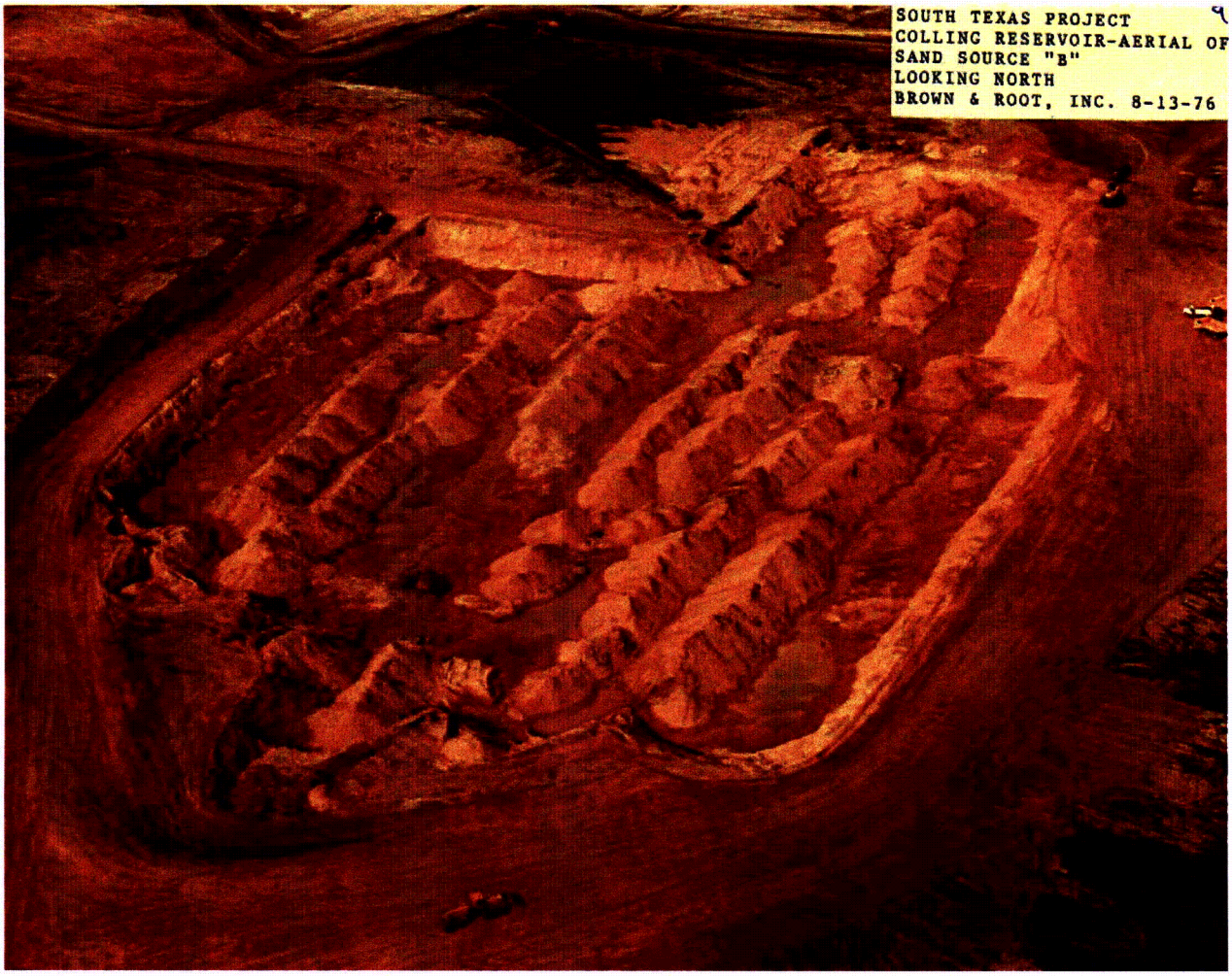

Figure 22. Sand deposits in the MCR near STP 3 & 4.

Figure 23. Sand layers and silt and clay layers in a trench near the MCR.

[Item 5] *Indicate if there are geologically conducive locations for the deposition and preservation of tsunami deposits at the STP site or nearby regions.*

In response to Item 5, no landslides have been documented at the location of the East Breaks slump in the last 10,000 years (Reference 9). Also, the maximum longitudinal extent of extreme run-up events occurring outside of enclosed bays is typically on the order of a few kilometers. For example, Reference 2 (p. 30) cites the maximum horizontal inundation in NGDC as 3.4 mi (5.5 km) for the December 26, 2004, Indian Ocean tsunami on the island of Sumatra.

In addition, Reference 15 provides calibrated historical sea level for the Northwestern Gulf of Mexico. As the East Breaks slump is estimated to be about 16,000 years old, sea level may have been at or near a 120-m, 120,000-year lowstand at the time of the slump. The head of the slump is also at the 120-m bathymetry contour relative to present day MSL (Figure 3). Therefore, if the slump produced a tsunami, geologic indicators would likely be present within a few kilometers of the East Breaks slump location.

Subsection 2.4S.6 will be replaced in its entirety in a future COLA update.

References:

1. Atlantic and Gulf of Mexico Tsunami Hazard Assessment Group, 2008, "Evaluation of Tsunami Sources with the Potential to Impact the U.S. Atlantic and Gulf Coasts - A Report to the Nuclear Regulatory Commission: U.S. Geological Survey Administrative Report," Revision: August 22, 2008.
2. Prasad, R., 2008, Tsunami Hazard Assessment at Nuclear Power Plant Sites in the United States of America, NUREG CR-6966, Pacific Northwest National Laboratory-17397, Nuclear Regulatory Commission, Draft Report for Comment, Revision: August 2008.
3. Borrero, J.C., Dolan, J.F. and C.E. Synolakis, 2001, Tsunamis Within the Eastern Santa Barbara Channel, Geophysical Research Letters 28(4): 643-646.
4. Borrero, J.C., 2002, "Tsunami Hazards in Southern California," Ph.D. Thesis, University of Southern California, 306 pp.
5. Titov, V.V. and Gonzalez, F.I., 1997, "Implementation and Testing of the Method of Splitting Tsunami (MOST) Model," National Oceanic and Atmospheric Administration, Technical Memorandum ERL Pacific Marine Environmental Laboratory (PMEL) 112.
6. Titov, V.V., and C.E. Synolakis, 1998, "Numerical Modeling of Tidal Wave Run-up," 1998, Journal of Waterway, Port, Coastal, and Ocean Engineering 124(4): 157-171.
7. Piper, J.N., and W.E. Behrens, 2003, Downslope Sediment Transport Processes and Sediment Distributions at the East Breaks, northwest Gulf of Mexico, in Proceedings of the 23rd Annual Gulf Coast Section SEPM Research Conference, Houston, TX, p. 359-385.
8. Hoffman, J.S., Kaluza, M.J., Griffiths, R., Hall, J. and T. Nguyen, 2004, "Addressing the Challenges in the Placement of Seafloor Infrastructure on the East Breaks Slide-A Case

Study: The Falcon Field (EB 579/623), Northwestern Gulf of Mexico," 2004, Offshore Technology Conference 16748.

9. Rothwell, R.G., Kenyon, N.H. and B.A. McGregor, 1991,"Sedimentary Features of the South Texas Continental Slope as Revealed by Side-Scan Sonar and High-Resolution Seismic Data," The American Association of Petroleum Geologists Bulletin 75(2): 298-312.

10. Winker, C.A. and J.S. Booth, 2000, Sedimentary Dynamics of the Salt-Dominated Continental Slope, Gulf of Mexico: Integration of Observations from the Seafloor, Near-Surface, and Deep Subsurface, GCSSEPM Foundation 20th Annual Research Conference, Houston, Texas, December 3-6, 2000, 1059-1086.

11. National Geophysical Data Center (NGDC), 2008, "GEODAS Grid Translator," National Oceanic and Atmospheric Administration (NOAA), available at http://www.ngdc.noaa.gov/mgg/gdas/gd_designagrid.html, accessed July 26, 2008.

12. Synolakis, C.E., Bardet, J.-P., Borrero, J.C., Davies, H.L., Okal, E.A., Silver, E.A., Sweet, S., and D.R. Tappin, 2002, "The Slump Origin of the 1998 Papua New Guinea Tsunami," Proceedings: Mathematical, Physical and Engineering Sciences 458(2020): 763-789.

13. Liu, P. L.-F., Lynett, P. and C. Synolakis, 2003, "Analytical solutions for forced long waves on a sloping beach," Journal of Fluid Mechanics 478: 101-109.

14. Locat, J., Lee, H.J., Locat, P., and J. Imran, 2004, "Numerical analysis of the mobility of the Palos Verdes debris avalanche, California, and its implication for the generation of tsunamis," Marine Geology 203: 269-280.

15. Simms, A.R., Anderson, J.B., Milliken, K.T., Taha, Z.P. and J.S. Wellner, 2007, "Geomorphology and age of the Oxygen isotope stage 2 (last lowstand) sequence boundary on the northwestern Gulf of Mexico continental shelf," in Davies, R.J., Posamentier, H.W., Wood, L. J. & Cartwright, J. A. (eds.), Seismic Geomorphology: Applications to Hydrocarbon Exploration and Production, Geological Society, London, Special Publications, 277: 29-46.

16. Gonzalez, F.I., Bernard, E., Dunbar, P., Geist, E., Jaffe, B., Kanoglu, U., Locat, J., Mofjeld, H., Moore, A., Synolakis, C.E., Titov, V. and R. Weiss (Science Review Working Group), 2007, "Scientific and Technical Issues in Tsunami Hazard Assessment of Nuclear Power Plant Sites," National Oceanic and Atmospheric Administration (NOAA) Technical Memorandum OAR Pacific Marine Environmental Laboratory 136.

17. Grilli, S.T. and P. Watts, 2005, Tsunami Generation by Submarine Mass Failure, Part I, Modeling Experimental Validation, and Sensitivity Analyses, Journal of Waterway, Port, Coastal, and Ocean Engineering 131(6): 283-297.

18. Watts, P., Grilli, S.T., Tappin, D.R. and G.J. Fryer, 2005, Tsunami Generation by Submarine Mass Failure, Part II, Predictive Equations and Case Studies, Journal of Waterway, Port, Coastal, and Ocean Engineering 131(6): 298-310.

RAI 02.04.06-2:

QUESTION:

Section C.I.2.4.6.3 of RG 1.206 provides specific guidance with respect to the source characteristics needed to determine the PMT. These characteristics include detailed geo-seismic descriptions of the controlling local and distant tsunami generators, including location, source dimensions, fault orientation, and maximum displacement. Provide these characteristics for seismogenic tsunamis originating in the Caribbean and Gulf of Mexico as used in the analysis. Also provide the location, source volume and dimensions, and maximum displacement information for landslides in the Gulf of Mexico used in the analysis.

RESPONSE:

The initial condition for Caribbean and Gulf of Mexico sources in Reference 2.4S.6-1 was based on the formulae of Okada (1985) (Reference below). For example, the seismogenic parameters for the Gulf of Mexico scenario (i.e., Reference 2.4S.6-1, p. 305) are provided in Table 1:

Table 1. Source parameters for Gulf of Mexico scenario in Reference 2.4S.6-1.

Epicenter	Mag. (M_w)	Rupture Length (km)	Width (km)	Depth (km)	Strike (deg)	Dip (deg)	Rake (deg)	Max slip (m)
20N, 265E	8.2	200	70	5	135	20	90	2

Reference 2.4S.6-1 (p. 305) states that all model sources were aligned with local strike.

The location, source volume and dimensions, and maximum displacement information for landslides in the Gulf of Mexico are discussed in the response to RAI 02.04.06-1.

No COLA revision is required as a result of this RAI response.

Reference:

Okada, Y., 1985, Surface deformation due to shear and tensile faults in a half-space, Bulletin of the Seismological Society of America 75(4): 1135-1154.

RAI 02.04.06-3:

QUESTION:

Section C.I.2.4.6.4 of RG 1.206 provides specific guidance with respect to tsunami analysis. This includes providing a complete description of the analysis procedure used to calculate tsunami wave height and period at the site. Provide available high-resolution processed radar data at and near the site as well as the source for the bathymetric dataset used for tsunami analysis.

RESPONSE:

A description of the analysis procedure used for the tsunami modeling at the STP Units 3 and 4 site is provided in the response to RAI 02.04.06-1.

Processed high-resolution bathymetric data is downloadable from the National Oceanic and Atmospheric Administration (NOAA) National Geophysical Data Center (NGDC) (Reference below). Specifically, the gridded dataset of the US Coastal Relief Model from the NGDC database (Reference below) is the source of the bathymetric, as well as topographic data for the tsunami analysis as shown in Figure 1.

No COLA revision is required as a result of this RAI response.

Reference:

National Geophysical Data Center (NGDC), 2008, "Bathymetry, Topography, and Relief," National Oceanic and Atmospheric Administration (NOAA), Available at http://www.ngdc.noaa.gov/mgg/bathymetry/relief.html, accessed October 5, 2008.

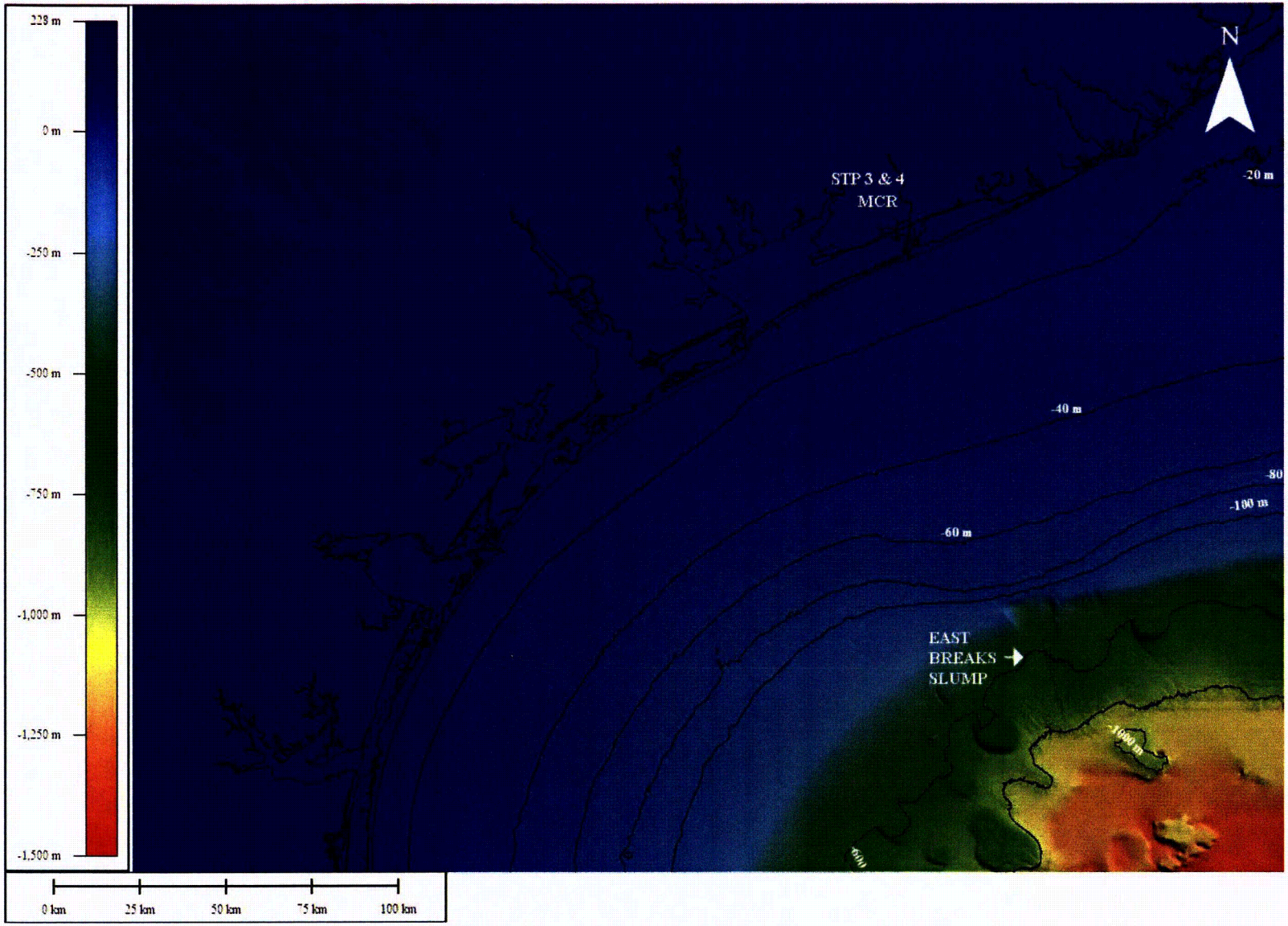

Figure 1. Six arc-second topography and bathymetry for the South Texas Coast and Gulf of Mexico (Source: Reference 1). Elevations are in units of meters and relative to NGVD29 (MSL).75